FROM A MULTI-REGION MODEL TO A MULTI-FLOW PATH MODEL: INTERPRETATION OF FLOW TESTS ON HETEROGENEOUS CORES

Christos A.Aggelopoulos[1,2] and Christos D. Tsakiroglou[1]

[1]Foundation for Research and Technology Hellas- Institute of Chemical Engineering and High Temperature Chemical Processes, Stadiou str., Platani, 26504 Patras, Greece
[2]Department of Physics, University of Patras, 26500 Greece

This paper was prepared for presentation at the International Symposium of the Society of Core Analysts held in Calgary, Canada, 10-12 September 2007

ABSTRACT

Immiscible and miscible displacement tests performed on long undisturbed soil columns are employed to quantify the soil heterogeneity at the macro- and micro- scale, respectively. The transient responses of the solute concentration (breakthrough curve) over three cross-sections are inverted by using a multi-region model to estimate the longitudinal dispersivity along with the variance of the microscopic permeability distribution (micro-heterogeneity). The transient responses of the total pressure drop across the soil column, and fluid saturation averaged over five successive segments are inverted by using a multi-flow path model to estimate the variance of the macroscopic permeability distribution (macro-heterogeneity) along with the tortuosity, and parameters quantifying the capillary pressure and relative permeability curves.

INTRODUCTION

Immiscible and miscible displacement experiments are commonly used to determine the two-phase flow and hydrodynamic dispersion coefficients of soils, respectively. The capillary pressure and relative permeability curves are estimated by inverting the transient responses of pressure drop and axial fluid saturation profile, whereas the hydrodynamic dispersion coefficients can be estimated by inverting the transient responses of solute concentration breakthrough curves (Tsakiroglou et al., 2005). The goal of the present work is to develop computational tools that will enable us to interpret the results of flow tests, not only by estimating the corresponding multiphase effective transport coefficients but also by quantifying the heterogeneity of soils at multiple scales.

EXPERIMENTAL SETUP

An experimental apparatus was constructed to measure the electrical conductance of disturbed and undisturbed sandy soils during immiscible and miscible displacement experiments. The apparatus consists of the sample holder, an in–house constructed multi-point conductivity meter, a HPLC pump, and a data-acquisition system installed in the host computer (Aggelopoulos and Tsakiroglou, 2005).

A core holder was constructed to perform flow tests on undisturbed soil columns. The undisturbed soil sample (length L=32.7 cm, diameter D=4.75 cm) is transferred carefully from the sampler into a rubber sleeve which is equipped with rod electrodes (Fig.1) and is closed by placing two composite caps on its ends. The entire system is placed inside an adjustable length cell body with the overburden pressure exerted on the sleeve to be slightly higher than the maximum pore pressure so that soil expansion and fluid leakages are avoided.

Two undisturbed soil columns (S3, S4) were collected from different depths of the unsaturated zone of an abandoned military airport, situated in North Poland and contaminated by jet fuel. Properties of soil columns: (S3) porosity ϕ=0.25, permeability k_0=50 mD, formation factor F=10.1; (S4) ϕ=0.25, k_0=142 mD and F=8.3. Before testing, each soil column was cleaned carefully by treating it with ethanol, methanol and toluene, and vice versa to ensure the removal of any traces of jet fuel.

INVERSE MODELING OF MISCIBLE DISPLACEMENT TESTS

BSEM images of pore casts (Fig.2a) and Hg injection tests (Fig.2b) have revealed that the pore structure of the investigated soils is characterized by a broad range of pore length scales spanning several orders of magnitude. In order to describe solute transport through such micro-scale heterogeneities (Fig.2a) a 2-parameter multi-region model was used.

A two-parameter multi-region model of miscible displacement

The pore space is regarded as an assemblage of intercommunicating parallel regions characterized by an area-based distribution of permeabilities $f_m\left(k_m^*;\sigma_{k_m^*}\right)$, where the dimensionless micro-scale permeability is defined as $k_m^* = k_m/k_0$, k_0 is the measured total permeability, and $\sigma_{k_m^*}$ is the standard deviation of the micro-scale permeability distribution function, and quantifies micro-scale heterogeneities (Fig.2). Solute dispersion in each region is described by the analytic solution of the 1-D advection-dispersion equation in homogeneous porous media (Tsakiroglou et al., 2005). The inter-communication between the various regions ensures that fluid pressure does not change over a cross-section and no convective solute transport occurs because of lateral pressure gradient. In addition, any lateral diffusive flux is also ignored. Under the abovementioned assumptions, the cross-sectional averaged solute concentration is given by

$$C^* = \int_0^\infty C_{k_m}^* f_m\left(k_m^*\right) dk_m^* \tag{1}$$

where the local solute concentration $C_{k\,m}^*$ is given by the analytic solution of the advection-dispersion equation. The local flow velocity and dispersion coefficient of each region vary according to the relations

$$u_{pk_m} = k_m^* u_{p0} \qquad D_{Lk\,m} = D_{eff} + \alpha_L u_{pk_m}{}^{m_a} \tag{2}$$

where u_{p0} is the mean pore velocity and D_{eff} the effective diffussivity. For macrodispersion, the exponent $m_a = 1$, and the multi-region model is quantified by two parameters: $\alpha_L, \sigma_{k_m^*}$. The Bayesian estimator of ATHENA Visual Studio 10 was used to estimate the longitudinal dispersivity, α_L, and $\sigma_{k_m^*}$ by fitting the predictions of the multi-region model simultaneously to solute breakthrough curves measured at three cross-sections of soils S3 & S4 (Table 1). The estimated dispersivity (Table 1) is comparable to corresponding values reported in literature (Roychoudhury, 2001); α_L is a measure of the length-scale of soil macro-heterogeneities, and changes weakly with flow velocity (Table 1).

The measured breakthrough curves are reproduced satisfactorily by the multi-region model (Fig.3a,b). It is worth mentioning the physical information embedded into the parameter values of the multi-region model. On the one hand, the dispersivity is indicative of the length-scale of macro-heterogeneities. On the other hand, the standard deviation of permeability distribution is indicative of the micro-heterogeneities associated with the variability of the pore length scales (Fig.2). In other words, miscible displacement experiments on undisturbed soils may be treated as a diagnostic tool of the soil heterogeneity and provide quantitative information about it.

INVERSE MODELING OF TWO-PHASE FLOW EXPERIMENTS

During rate-controlled immiscible displacement experiments on both soil columns S3 and S4, oil breakthrough occurred very fast, and the variation of water saturation in the lower segments of the soil column was quite small, and very difficult to be detected precisely. Oil moves along preferential flow paths and most of the water is bypassed, resulting in a high value of "irreducible" wetting phase saturation. In order to account for such characteristics of the 3-D flow field the multi-flow path model was adopted.

Multi-flow path model

The broad range of pore length scales probed in undisturbed soils (Fig.2), induces the creation of highly permeable (critical) pathways which transfer most of the flow and control the permeability and electrical conductivity of the soil (Tsakiroglou et al., 2006). These flow pathways exhibit the smallest capillary resistance to the invasion of the non-wetting fluid (oil) and hence they also act as preferential oil flow paths during drainage. The pore space is represented by a system of flow paths characterized by a distribution of macro-scale permeability, $f_M\left(k_M^*;\Sigma_{k_M^*}\right)$. The standard deviation, $\Sigma_{k_M^*}$, is a measure of the soil macro-heterogeneity, as it indicates the degree of uniformity among the various flow paths. Each flow path contains a sub-set of the regions mentioned earlier (multi-region model), and its permeability is governed by the permeability distribution over this sub-set. The flow paths are neither straight nor perpendicular to the main flow direction, and their mean length L_{fp} is defined by a common tortuosity factor, $\lambda = L/L_{fp}$, where L is the soil core length. The oil/water displacement in each flow path is regarded as

frontal and is described by the irreducible wetting phase saturation, S_{wi}, and end oil relative permeability $k_{ro}^{0} = k_{ro}(S_w = S_{wi})$. In order to compute the capillary pressure of displacement in each flow path, a 2-parameter Leverett type equation of the form

$$P_c(k) = (c\gamma_{ow}\cos\theta)k_M^{-\delta} \tag{3}$$

was used. Using mass and momentum balances, oil/water displacement was described by a system of integral & differential equations with dependent variables the total pressure drop, $\Delta P_t^*(\tau)$ and the positions, $\xi_f(k_M^*)$ of interfaces (fronts) along flow paths. This approach is analogous to earlier ones developed for simulating the two-phase flow in a disordered system of parallel capillary tubes (Bartley and Ruth, 1999; Dong et al., 2006). Using Athena Visual Studio 10, the measured transient responses of the water saturation profile and total pressure drop were fitted with the multi-flow path model in order to estimate all pertinent parameters. The system of equations is solved iteratively by using the Simpson method to integrate the pressure drop over all flow paths and a 4th order Runge-Kutta to calculate the axial position of interfaces as a function of time. It is evident that the macro-heterogeneity (Table 2) is much weaker than micro-heterogeneity (Table 1). The transversely averaged fluid saturation calculated at the current axial positions of the interfaces (fronts), $\xi_f(k_M^*)$, was plotted versus the corresponding capillary pressures $P_c^*(k_M^*)$, Eq.(3), to compute $P_c(S_o)$. Respectively, the relative permeabilities as functions of the current positions of the fronts in flow paths, $\xi_f(k_M^*)$, were calculated by using the relationships

$$k_{ro}(\xi_f) = k_{ro}^{0}\int_{k_M^*(\xi_f)}^{k_{M,\max}^*} k_M^* f_M^*(k_M^*)dk_M^* \quad k_{rw}(\xi_f) = \int_{k_{M,\min}^*}^{k_M^*(\xi_f)} k_M^* f_M(k_M^*)dk_M^* \tag{4}$$

The low levels of oil saturation measured over the lower segments are comparable to the resolution of the technique and for this reason a discrepancy is observed between experiment and theoretical prediction (Fig.4). The capillary pressure and relative permeability curves estimated by the multi-flow path model are shown in Fig.5.

REFERENCES

1. Aggelopoulos, C., and C.D. Tsakiroglou, "Simultaneous determination of the two-phase flow and hydrodynamic dispersion coefficients of soils from transient immiscible and micible displacement experiments", *Proceeding of the 2005 Annual Symposium of the Society of Core Analysts*, Paper SCA2005-58, Toronto, Canada, 21-25 August 2005.
2. Bartley, J.T. and D.W. Ruth, "Relative permeability analysis of tube bundle models", *Transp. Porous Media* (1999) **36**, 161-187.
3. Dong, M., F.A.L. Dullien, L. Dai, and D. Li, "Immiscible displacement in the interacting capillary bundle model. Part II. Applications of model and comparison of interacting and non-interacting capillary bundle model", *Transp. Porous Media* (2006) **63**, 289-304.

4. Roychoudhury, A.N., "Dispersion in unconsolidated aquatic sediments", *Estuar. Coast. Shelf. S.* (2001) **53**, 745-757.
5. Tsakiroglou, C.D., M.A. Theodoropoulou, V. Karoutsos, and D. Papanicolaou, "Determination of the effective transport coefficients of pore networks from transient immiscible and miscible displacement experiments", *Water Resources Research*, (2005) **41**, W02014.
6. Tsakiroglou, C.D., M.A. Ioannidis, E. Amirtharaj, O. Vizika, "A new approach for the characterization of the pore structure of dual porosity rocks", *Proceeding of the 2006 Annual Symposium of the Society of Core Analysts*, Paper SCA2005-24, Trondheim, Norway, 12-16 Sept. 2006.

ACKNOWLEDGEMENTS

This work was performed under Global Change and Ecosystems contract number SSPI-CT-2003-004017-STRESOIL (2004-2007) supported by the European Commission.

Table 1. Estimated parameter values of the multi-region model

u_{p0} (m/s)	Soil column S3		Soil column S4	
	α_L (cm)	$\sigma_{k_m^*}$	α_L (cm)	$\sigma_{k_m^*}$
1.50e-6	2.96	1.40	-	-
2.63e-6	4.0	2.36	9.67	1.59
3.76e-6	1.20	1.34	5.96	1.70
5.26e-6	1.74	1.24	6.01	1.48
7.52e-6	-	-	5.26	0.86
9.40e-6	2.23	0.90	3.72	1.04

Table 2. Estimated parameter values of the multi-flow path model

Parameter	Soil S3	Soil S4
$\Sigma_{k_M^*}$	0.16	0.07
λ	0.88	1.0
c	$1.2\text{x}10^{-3}$	$4.7\text{x}10^{-4}$
δ	0.70	0.72
S_{wi}	0.57	0.56
k_{ro}^0	0.6	0.51

Figure 1. Rubber sleeve with soil column and built-in rod electrodes.

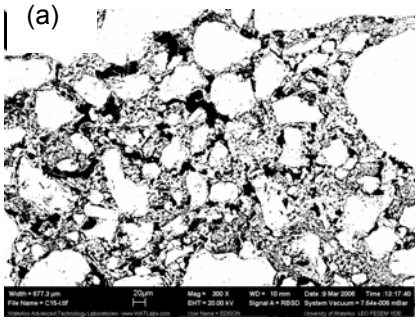

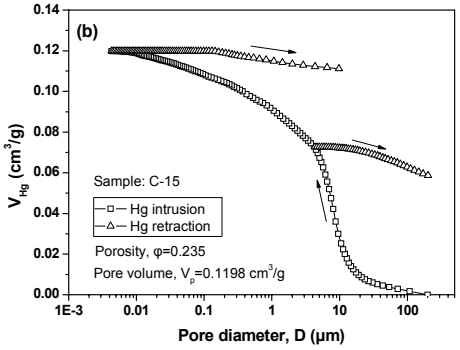

Figure 2. (a) BSEM image (magnification=300x) of the 2-D cross-section of sample C15 originating from the same zone with that of soil column S4. (b) Hg intrusion / retraction curves of sample C15

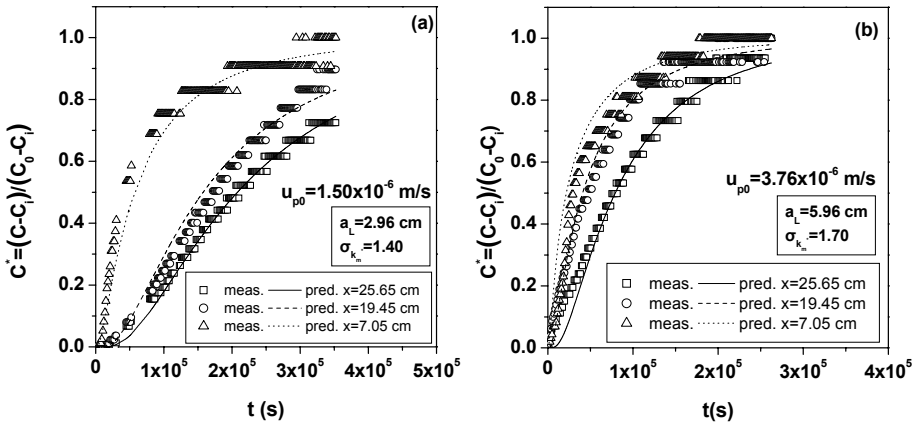

Figure 3. Experimentally measured vs theoretically predicted (multi-region model) solute concentration breakthrough curves at various mean pore velocities for (a) soil S3, (b) soil S4.

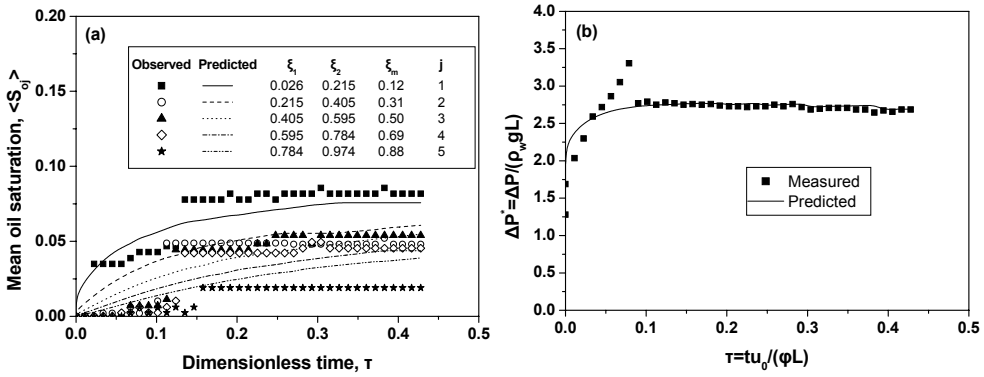

Figure 4. Numerically predicted vs experimentally measured (a) axial saturation profiles, (b) pressure drop across the soil column.

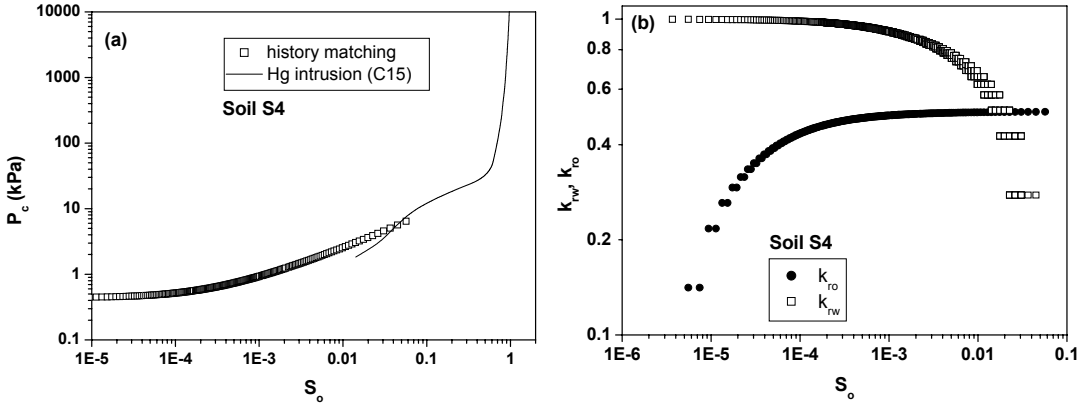

Figure 5. (a) Estimated capillary pressure curve vs oil/water capillary pressure curve resulting from Hg intrusion data. (b) Estimated relative permeability curves.